PNAS RESEARCH ARTICLE | ECOLOGY
EARTH, ATMOSPHERIC, AND PLANETARY SCIENCES

Space weather disrupts nocturnal bird migration

Eric R. Gulson-Castillo[a,b], Benjamin M. Van Doren[c], Michelle X. Bui[d,1], Kyle G. Horton[e], Jing Li[f,2], Mark B. Moldwin[g], Kerby Shedden[f], Daniel T. Welling[g], and Benjamin M. Winger[a,b,3]

Edited by Pablo Marquet, Pontificia Universidad Catolica de Chile, Santiago, Chile; received April 18, 2023; accepted August 22, 2023

Space weather, including solar storms, can impact Earth by disturbing the geomagnetic field. Despite the known dependence of birds and other animals on geomagnetic cues for successful seasonal migrations, the potential effects of space weather on organisms that use Earth's magnetic field for navigation have received little study. We tested whether space weather geomagnetic disturbances are associated with disruptions to bird migration at a macroecological scale. We leveraged long-term radar data to characterize the nightly migration dynamics of the nocturnally migrating North American avifauna over 22 y. We then used concurrent magnetometer data to develop a local magnetic disturbance index associated with each radar station (ΔBmax), facilitating spatiotemporally explicit analyses of the relationship between migration and geomagnetic disturbance. After controlling for effects of atmospheric weather and spatiotemporal patterns, we found a 9 to 17% decrease in migration intensity in both spring and fall during severe space weather events. During fall migration, we also found evidence for decreases in effort flying against the wind, which may represent a depression of active navigation such that birds drift more with the wind during geomagnetic disturbances. Effort flying against the wind in the fall was most reduced under both overcast conditions and high geomagnetic disturbance, suggesting that a combination of obscured celestial cues and magnetic disturbance may disrupt navigation. Collectively, our results provide evidence for community-wide avifaunal responses to geomagnetic disturbances driven by space weather during nocturnal migration.

bird migration | space weather | geomagnetic disturbances | radar

Earth's magnetic field is occasionally but regularly impacted by bursts of energy from the Sun ("space weather"), such as coronal mass ejections (1, 2) (Fig. 1*A*). On Earth, the impact of larger geomagnetic disturbances caused by space weather includes the auroras as well as geomagnetic storms that disrupt satellite communications, navigation systems, and power grids (2, 3). Despite the magnitude of interference that large geomagnetic disturbances can have on human-built technology, less is known about how geomagnetic disturbances affect biological systems, including animals that depend on Earth's magnetic field for migratory orientation and navigation.

That animals use Earth's magnetic fields for orientation and navigation has been decisively shown through decades of observation and experimentation (5, 6). There is strong evidence that birds, sea turtles, and other organisms depend on magnetic information at multiple spatial scales, keying into small changes in inclination, intensity, and declination when making orientation decisions and developing navigational maps (7–10). Experimental evidence that birds alter navigation decisions based on minor changes in the local magnetic field (7, 11) suggests that large space weather events could potentially disrupt the ability of migrating animals to navigate. However, evidence of impacts from naturally occurring disturbances on free-roaming animals is scarce. Previous studies in migratory birds have suggested potential correlations between geomagnetic disturbances and changes in dispersion patterns of bird headings (12), changes in migratory routes (13) or arrival patterns after oceanic crossing (14), shifts in pigeon homing direction (15, 16), increases in bird vagrancy (17), and decreased expression of migratory restlessness in captivity (18). Other studies have reported relationships between sunspot counts—a correlate of increased solar activity and space weather—and both cetacean beach strandings (19) and pigeon homing efficiency (20). However, such studies have been relatively localized in geographic, temporal, or phylogenetic scale, often focusing on specific migration observatories or single species (but see ref. (17)). Additionally, some previous results have been inconsistent or contradictory, such as those using bird headings and homing pigeons (21, 22), highlighting how little is known of how animal navigation is affected by geomagnetic disturbances, especially at landscape and population scales.

Here, we leverage long-term ecological and geomagnetic datasets at a macroecological scale to test how nocturnally migrating birds in a continental flyway interact with the

Significance

Birds and other animals depend on Earth's magnetic field for long-distance navigation during their seasonal migrations. However, the magnetic field is regularly disrupted by bursts of solar energy, which may temporarily decrease its reliability for navigation. We used long-term datasets derived from Doppler radar and magnetometers to test whether geomagnetic disturbance is correlated with the number of birds migrating, their effort flying against the wind, and their flight altitude. Our results suggest that fewer birds migrate during strong geomagnetic disturbances and that migrating birds may experience more difficulty navigating, especially under overcast conditions in autumn. Our results provide ecological context for decades of research on the mechanisms of animal magnetoreception by demonstrating community-wide impacts of space weather on migration dynamics.

Author contributions: E.R.G.-C. and B.M.W. designed research; E.R.G.-C., B.M.V.D., M.X.B., K.G.H., M.B.M., and D.T.W. performed research; E.R.G.-C., B.M.V.D., M.X.B., K.G.H., J.L., K.S., and D.T.W. analyzed data; B.M.V.D., K.G.H., M.B.M., and D.T.W. edited and commented on the paper; and E.R.G.-C. and B.M.W. wrote the paper.

The authors declare no competing interest.

This article is a PNAS Direct Submission.

[1]Present address: Department of Earth and Atmospheric Sciences, Cornell University, Ithaca, NY 14850.

[2]Present address: Department of Biostatistics, University of Michigan, Ann Arbor, MI 48109.

[3]To whom correspondence may be addressed. Email: wingerb@umich.edu.

This article contains supporting information online at https://www.pnas.org/lookup/suppl/doi:10.1073/pnas.2306317120/-/DCSupplemental.

Published October 9, 2023.

dynamism of the magnetosphere. Weather surveillance radars capture community-wide dynamics of nocturnal migration, providing detailed measurements of migration intensity and direction over the United States' NEXRAD network (23–26). We use a 23-y (1995 to 2018) dataset on bird migration collected from 37 radar stations in the central migration flyway of the US Great Plains, a major migratory corridor (Fig. 1*B*). We specifically chose this relatively flat region to minimize variation in migratory orientation caused by mountainous topography or oceanic and Great Lakes coastlines (27, 28). The community of nocturnally migrating birds in this region is primarily composed of a diverse set of perching birds (Passeriformes; 73% of species), shorebirds (Charadriiformes; 12%), and waterfowl (Anseriformes; 9%) (29). We then matched data from each radar station with a customized, spatiotemporally explicit index of geomagnetic disturbance, ΔBmax, which represents the maximum hourly change in nanoTeslas (nT) from background magnetic conditions (*Materials and Methods*). We derived ΔBmax from time series of geomagnetic measurements collected from magnetometer stations near the focal radar stations (Fig. 1*B* and *SI Appendix*, Figs. S1 and S2 and Table S1) (30). These local data, which we accessed from the superMAG database (31), are processed to remove daily and seasonal fluctuations, leaving only variations caused by space weather effects (*Materials and Methods*). As the dynamics of nocturnal bird migration are greatly affected by atmospheric weather conditions (26, 32), we model the impact of geomagnetic disturbances on bird migration while controlling for the expected effects of atmospheric weather (*Materials and Methods*).

We hypothesized that geomagnetic disturbances hinder effective orientation and navigation during migration. Specifically, we predicted decreases in nocturnal migration intensity—the quantity of migrating birds—during high geomagnetic disturbance as a consequence of increased hesitancy to initiate or continue migration with unstable navigation cues. We also predicted decreased effort flying against the wind, hypothesizing that birds migrating under strong magnetic disturbances will spend less effort actively navigating in flight and consequently fly in greater alignment with the wind. We further predicted that any effects of geomagnetic disturbances on migratory parameters should be magnified when other navigation cues are obscured, specifically under overcast conditions, which can obstruct nocturnally migrating birds' abilities to see celestial cues (33, 34). Finally, a previous study found evidence for decreases in the altitude at which migrating birds fly in response to a geographic magnetic anomaly, potentially to be closer to terrestrial landmarks or to follow changing magnetic field parameters (35), so we additionally tested whether similar decreases in mean altitude occurred in response to space weather geomagnetic disturbances.

Results and Discussion

Modeling Framework. We used two complementary methods to quantify the influence of geomagnetic disturbances on migration response variables while accounting for complex spatial and temporal autocorrelation with atmospheric weather predictors. First, our "global" nonlinear mixed effects (NLME) models include all predictors and produce CI simulated from model error parameters (36, 37). These models successfully recovered previously documented relationships between migration response variables and atmospheric weather and spatiotemporal predictors (23, 32)

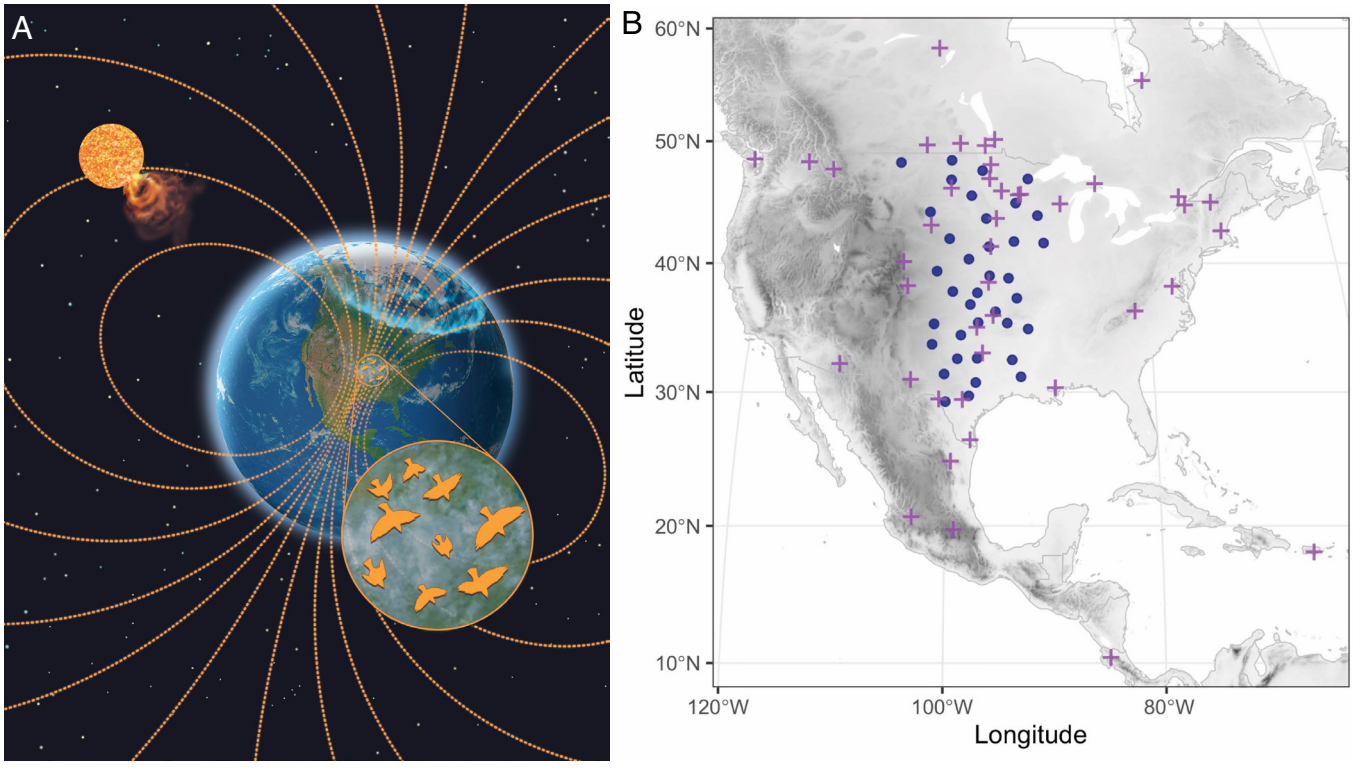

Fig. 1. Conceptual and geographic layout of our study system. (*A*) Space weather from the Sun, such as coronal mass ejections, disturbs Earth's magnetic field, causing the auroras and potentially decreasing the magnetic field's reliability for migrating birds. Artwork by John Megahan. (*B*) Distribution of NEXRAD radar stations (dark blue circles) and SuperMAG inventory magnetometer stations (purple crosses) used in this study in relation to topography (grayscale) (4). We used the three closest and active magnetometer stations surrounding each radar station (*SI Appendix,* Fig. S1) to interpolate ΔBmax, or maximum change in the magnetic field from quiet conditions, every hour. Some magnetometer stations had periods of missing data (*SI Appendix,* Fig. S2 and Table S1), so we sampled magnetometers from a larger geographical area than the radar stations to achieve a robust time series.

(*SI Appendix*, Figs. S3–S8), providing confidence in their predictive abilities in this complex dataset. Our second statistical framework uses machine learning decision tree (MLT) models to residualize our response variables against the weather and spatiotemporal variables (38). MLT models have been previously used to produce accurate predictions of migration in response to these variables (26), and thus, residuals reflect variance not explained by weather and spatiotemporal variables. The MLT residualization process excludes ΔBmax, and in models testing an interaction between ΔBmax and cloud cover, it also excludes cloud cover. We then tested for an effect of ΔBmax and cloud cover on the residuals using nonlinear regression and covariance matrix-estimated confidence bands (39, 40). Full modeling details are provided in *Materials and Methods*.

We assessed the support for model trends by comparing CI at the median ΔBmax value for each season (noted as $\Delta Bmax_{17\ nT}$, the same for both seasons) and the highest ΔBmax value for a particular measurement (ranging from 1,690 to 1,870 nT, depending on the occurrence of geomagnetic disturbances under varying circumstances, noted as e.g., $\Delta Bmax_{1690\ nT}$). We interpret nonoverlapping and narrow CI at these points as showing support for a trend, and we verified these CI through visualization of the model predictions. NLME comparisons are not centered around 0 because they result from conditional effect predictions, so changes in bird behavior at high ΔBmax are relative to predictions from low ΔBmax. As such, both numbers may be positive, even if the model predicts decreases.

Migration Intensity and Geomagnetic Disturbance. Our models generally recovered support for a relationship between large geomagnetic disturbances (ΔBmax) and decreased migration intensity. Migration intensity decreased at large-magnitude geomagnetic disturbances by 11.2% in our spring MLT residuals model (Fig. 2*A* and *SI Appendix*, Fig. S9; 95% CI $\Delta Bmax_{17\ nT}$: −0.001, 0.000, $\Delta Bmax_{1724\ nT}$: −0.19, −0.03). Consistent with this trend, our spring NLME model predicted a 17.4% reduction in migration intensity at high ΔBmax (Fig. 2*B*), although support was slightly weaker in the NLME model as CI at the median and highest ΔBmax overlap partially (Fig. 2*B*; 95% CI $\Delta Bmax_{17\ nT}$: 2.88, 3.106, $\Delta Bmax_{1724\ nT}$: 2.68, 2.96). In the fall, our MLT residuals model predicted an 8.9% decrease in migration intensity at high ΔBmax (Fig. 2*C* and *SI Appendix*, Fig. S10; 95% CI $\Delta Bmax_{17\ nT}$: −0.0003, 0.001, $\Delta Bmax_{1873\ nT}$: −0.14, −0.03). These three models predicted decreases in migration intensity at geomagnetic disturbances greater than ~500 nT (Fig. 2). By contrast, our fall NLME model had low support for a relationship between migration intensity and ΔBmax (Fig. 2*D*).

The decreases in migration intensity predicted by our models suggest that birds are less likely to initiate or continue migration under unstable geomagnetic conditions. Such a relationship suggests that geomagnetic disturbances may make the magnetic field less reliable for birds, affecting their decision to migrate. This idea is consistent with experimental simulations of geomagnetic disturbances that found decreases in migratory restlessness in some species (18). However, our models with an interaction between ΔBmax and cloud cover did not consistently recover changes in migration intensity at high ΔBmax and overcast conditions in either season (*SI Appendix*, Figs. S11–S14), suggesting that geomagnetic disturbances do not have a stronger effect on the overall number of migrating birds under overcast conditions, contrary to our predictions.

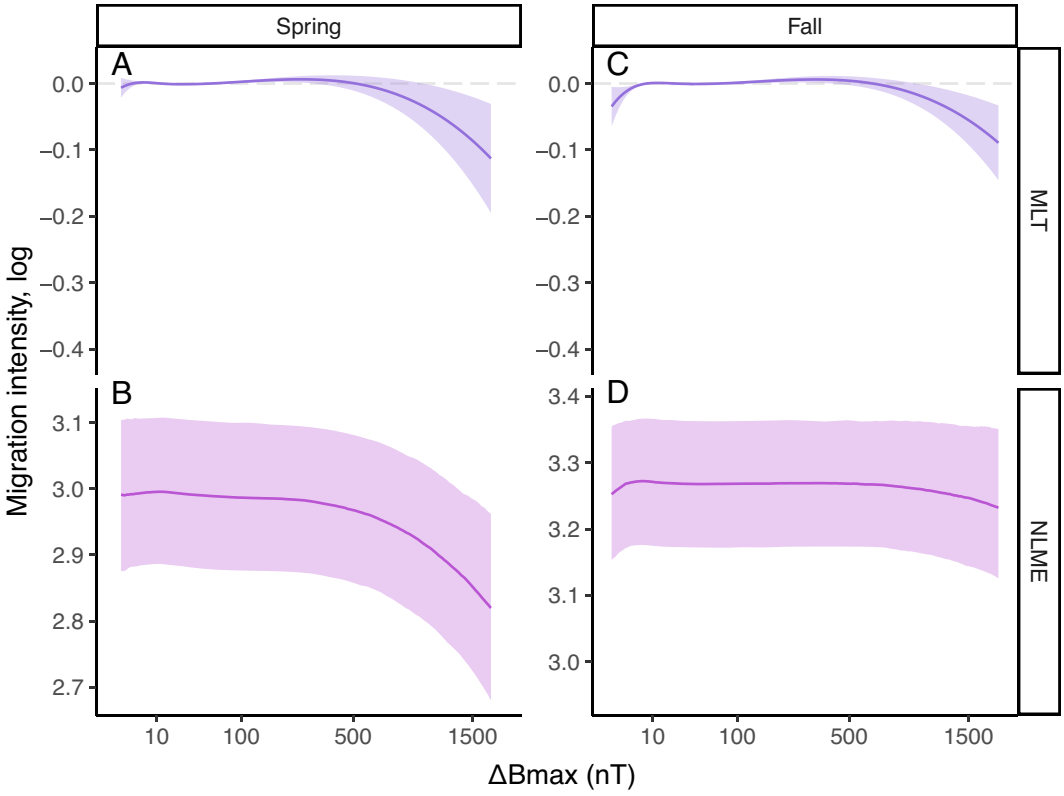

Fig. 2. Migration intensity predictions with geomagnetic disturbances. (*A*) Our MLT residual model and (*B*) NLME model predict decreases of 11% and 17%, respectively, in migration intensity at high geomagnetic disturbance (ΔBmax) in the spring. (*C*) Our MLT residual model predicts migration intensity decreases of 9% at high ΔBmax in the fall, but the corresponding NLME model (*D*) does not recover a similarly strong relationship. The spring models and the fall MLT residual model begin predicting decreased migration intensity with geomagnetic disturbances of around 500 nT.

Effort Flying against the Wind and Geomagnetic Disturbance. To test whether birds' active navigation decreased during geomagnetic disturbances, we assessed the impact of geomagnetic disturbances on the crosswind component of bird airspeed. Here, the crosswind component is the vector component of bird flight, or the flight energy, that is perpendicular to the wind vector and represents effort flying against the wind. We predicted that birds migrating under large geomagnetic disturbances would not navigate as effectively and would drift more with the wind, decreasing their crosswind component. We found the main effect of ΔBmax to be associated with a decrease of the crosswind component only in the fall MLT residuals model (*SI Appendix*, Fig. S15). This relationship was best supported at high but not extreme ΔBmax values (*SI Appendix*, Fig. S15; predicted decrease of 1.7%; $\Delta Bmax_{1000\ nT}$: −0.030, -0.004). Our models did not find changes in the crosswind component in response to ΔBmax in the fall NLME model (*SI Appendix*, Fig. S16) or in either spring model (*SI Appendix*, Figs. S15 and S16), weakening support for a relationship between a main effect of ΔBmax and the crosswind component. Yet, when we tested for an interaction between cloud cover and ΔBmax, our fall NLME model predicted a 25.4% decrease in the crosswind component at 100% cloud cover and high ΔBmax (Fig. 3*B*; 95% CI $\Delta Bmax_{17\ nT}$: 0.48, 0.54; $\Delta Bmax_{1694\ nT}$: 0.16, 0.34). The MLT residuals model also showed a 7.6% decrease under those circumstances, but this relationship has lower support from model CI (*SI Appendix*, Fig. S17; 95% CI $\Delta Bmax_{17\ nT}$: −0.007, −0.002; $\Delta Bmax_{1694\ nT}$: −0.215, 0.054). Evidence for decreases in effort flying against the wind with overcast conditions and large geomagnetic disturbances during fall is consistent with our hypothesis that migrating birds have difficulty navigating during geomagnetic disturbances while other navigation cues are obscured (33, 34). That is, birds aloft during geomagnetic disturbances in the fall may end up drifting with the wind more often. This interpretation aligns with research showing that birds drift with the wind upon sudden release at migratory altitudes under cloudy conditions, whereas they fly in the expected migratory direction against the wind under clearer conditions (41).

Interestingly, we only found relationships between ΔBmax and the crosswind component in the fall, whereas in the spring none of the models showed well-supported trends (Fig. 3*A* and *SI Appendix*, Fig. S18). Notably, a recent study on the relationship between geomagnetic disturbances and bird vagrancy—individuals appearing outside of their expected seasonal range—also found effects only in the fall (17). These patterns could be linked if birds migrating under conditions faulty for navigation are thrown off course by the wind and become vagrants. Our radar measurements of fall migration include many inexperienced juveniles migrating for the first time, whereas spring migration is composed of birds that have completed at least one leg of a migratory round trip. Therefore, the differences in spring versus fall patterns shown here may be a consequence of a more disruptive effect of magnetic disturbance on the migration of inexperienced, young birds (7) which are thought to depend on simpler "clock and compass" magnetic orientation strategies rather than the "true" magnetic map navigation displayed by experienced migrants (5, 42–44). There may be other nonexclusive explanations for these seasonal differences, all of which require further research. The well-documented faster pace of spring versus fall migration, which is thought to be driven by competition for nesting sites and phenological demands (45–47), may select for greater effort flying against the wind in spring than fall, regardless of magnetic conditions. Additionally, prior work proposes that birds may allow for more drift if they are far from their destination and compensate for drift as they approach their goal (48). This idea is in line with the seasonal differences that we detect here because in spring long-distance Neotropical migrants observed within our study region are likely closer to their destinations than they are in fall. Finally, at the mid-latitudes that encompass our study area, large geomagnetic storms cause local decreases in the magnetic field strength (49), although

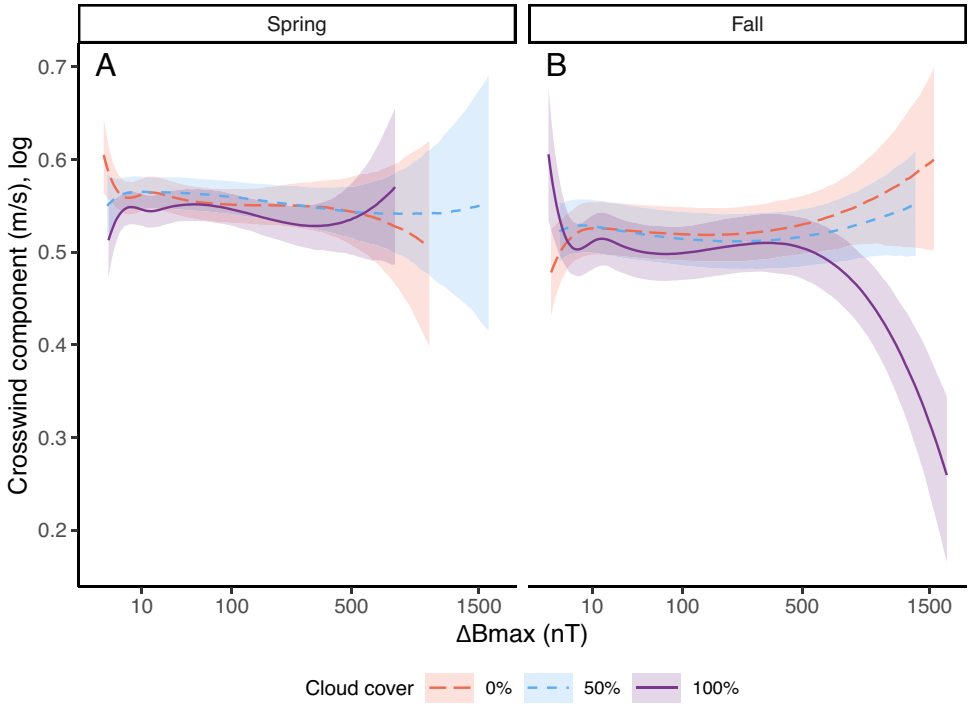

Fig. 3. Crosswind component of airspeed predictions with geomagnetic disturbances at different cloud cover levels. (*A*) Our spring NLME model does not predict changes in the crosswind component with magnetic disturbance or different cloud cover levels. (*B*) Our fall NLME model predicts a 25% decrease in effort flying against the wind at high ΔBmax and 100% cloud cover. The model otherwise predicts no changes in the crosswind component during geomagnetic disturbances at lower cloud covers.

exceptions occur due to auroral and other currents (50). When the local magnetic field strength decreases, it could temporarily mimic the magnetic field from further south, potentially causing complex seasonal differences in how birds respond to geomagnetic disturbances.

Flight Altitude and Geomagnetic Disturbance. We found little support for an effect of geomagnetic disturbances on the mean altitude of migrants aloft. In both seasons, models that included only a direct effect of ΔBmax on mean altitude did not suggest a general relationship between migration altitude and geomagnetic disturbances (*SI Appendix*, Figs. S19 and S20). Models with an interaction between cloud cover and ΔBmax also did not broadly suggest interacting effects under overcast conditions (*SI Appendix*, Figs. S21–S24). These results contrast with decreases in altitude observed over a different magnetic stimulus, a geographic magnetic anomaly (35), which may have enabled recognition of terrestrial landmarks or have been a product of birds following shifts in inclination isoclines. The nature of these disturbances is also different, as the magnetic anomaly was associated with an increase in magnetic field strength (35) while geomagnetic storms generally involve decreases in magnetic field strength (49). Our results suggest that navigating birds may respond differently to geographic magnetic anomalies versus temporal disturbances caused by space weather.

Comparison between Atmospheric Weather and Space Weather. Our NLME models allowed us to estimate the effects on response variables of each weather and spatiotemporal predictor and therefore compare their relative impact with geomagnetic disturbances. Consistent with our understanding of migration biology, the biggest environmental impacts on migration intensity that we detected were associated with atmospheric weather and spatiotemporal variables (23, 32). For example, with all other variables held equal, warm temperatures in the spring were associated with a 45.2% increase in migration intensity compared to the mean temperatures (*SI Appendix*, Fig. S4; 95% CI $_{6\,°C}$: 2.88, 3.10; $_{20\,°C}$: 3.33, 3.55) and north winds in the fall were associated with an around 43.1% increase in migration intensity compared to south winds (*SI Appendix*, Fig. S3; 95% CI $_{-20\,m/s}$: 3.38, 3.57; $_{20\,m/s}$: 2.95, 3.14). Despite the smaller magnitude of the effects of ΔBmax that we detect on bird migration compared to atmospheric weather, log-likelihood tests of NLME models supported the inclusion of ΔBmax and an interaction with cloud cover, with only three exceptions, even when CI indicated low support for predicted trends (*SI Appendix*, Table S2).

Conclusions. Our study provides correlational evidence for a relationship between nocturnal bird migration dynamics and geomagnetic disturbances. Importantly, our analyses explicitly controlled for the effects of atmospheric weather instead of examining geomagnetic disturbance in isolation, which has been a limitation of previous studies (12, 13, 15–17), (but see ref. 14). We found broad support that migration intensity decreases under high geomagnetic disturbance. However, we found that an interaction between cloud cover and geomagnetic disturbance did not affect migration intensity and was apparently only important for one variable, the crosswind component in the fall. These results suggest that the decision to migrate or not during geomagnetic disturbances is not generally affected by the ability to see celestial cues, but that navigation might be impaired under those conditions if birds decide to migrate.

Our analyses further suggest that correlations between migration dynamics and geomagnetic disturbance are mostly evident with the largest geomagnetic disturbances in our dataset, specifically those that had variations larger than ~500 nT (e.g., Figs. 2 and 3). These large disturbances occurred on 81 (3.32%) unique nights in the fall and 50 (2.28%) unique nights in the spring in our 23-y dataset. Incidences of this magnitude are thought to be caused by space weather and solar activity (51, 52). Therefore, although the frequency of such events is relatively low, our results nevertheless strengthen the link between extraterrestrial impacts on the Earth's magnetic field and the behavior of nocturnally migrating birds. Indeed, 75.5% of the large disturbances included in our dataset are directly linked to registered geomagnetic storms and all are associated with high planetary magnetic activity (*SI Appendix*, Table S3) (53).

Our findings highlight how animal decisions are dependent on environmental conditions—including those that we as humans cannot perceive, such as geomagnetic disturbances—and that these behaviors influence population-level patterns of animal movement. Our finding that geomagnetic disturbances might impact both the number of birds migrating and their directionality strengthens previous suggestions of the effects of geomagnetic disturbances on bird migration (12, 17, 18). By leveraging the massive amount of data collected by radar and magnetometer stations, we were able to detect and quantify larger-scale patterns than previously possible. Finer-scale patterns, such as species-specific responses or interactions with life history traits, cannot be studied with our current dataset but remain a promising topic of future research, perhaps in combination with citizen science projects or bird banding efforts (17, 29). Traits that vary across birds that migrate at night through our study area (e.g., Passeriformes, Anseriformes) include body size, migration distance, and development of migration routes through social learning versus genetic inheritance (54), all of which could affect susceptibility to geomagnetic disturbances. Our work further implies that longer-term impacts to Earth's magnetic field could also affect bird migration, such as the 11-y solar cycles that affect the frequency of geomagnetic disturbances (55). Further development of migration monitoring technology will allow for expansions in our understanding of how space weather and changes in the magnetosphere interact with biological systems.

Materials and Methods

Nocturnal Migration. To characterize nocturnal migration, we sampled NEXRAD scans that are made every 5 to 10 min to extract measures approximately every 30 min, and we used scans beginning after sunset and ending before sunrise (average fall 22.53 scans/night, spring 20.44 scans/night). Data were downloaded from the Amazon Web Services repository (https://s3.amazonaws.com/noaa-nexrad-level2/index.html). We used data from spring and fall migration periods from the nights of 1 March to 1 June and 1 August to 15 November (26). For each radar sampling event, we built vertical profiles of migration intensity (from reflectivity) and migrant speed and direction (from radial velocity) at 100 m intervals between 100 m and 3,000 m above ground level (56). We used data out to a 100-km radius in the construction of these profiles and elevation scans below 5.0°. For these profiles of migrant behavior, we removed precipitation contamination using the MistNet algorithm (57). MistNet is a convolutional neural network that classifies individual sampling volumes as biological or nonbiological.

We used three response variables that measure the mean behavior of birds flying over radar stations. We characterized migration intensity from radar reflectivity (η, cm^2/km^3), which measures bioscatter and correlates strongly with the number of birds migrating, that is, the intensity of bird migration (58). Mean altitude or elevation (km) is the distance above the ground at which most birds are detected in the air column. The crosswind component of airspeed (m/s) is the vector component of the bird airspeed vector positioned perpendicular to the wind vector. It quantifies the extent to which a bird is flying against the wind, with smaller values resulting from greater alignment with the wind. To calculate this, we multiplied the airspeed vector by the sine of the angle between the airspeed

vector and the wind vector. If this angle was larger than 90°, we subtracted it from 180° before taking the sine.

To simplify statistical analyses, we summed values of migration intensity across the vertical profile for each radar scan and then took the base-10 logarithm. For altitude, we used mean altitude weighted by migration intensity across 100-m vertical intervals. For the crosswind component, we used mean crosswind component weighted by migration intensity across 100-m vertical intervals for each radar scan and took the logarithm after adding 0.001 as a correction for observations for which the crosswind component was 0 m/s. Prior to summarizing our data, we excluded height bins with missing measurements for migratory intensity and bird direction. We excluded 2,202 radar scans in which more than 16 of 30 vertical intervals were missing data. After summarizing our data, we excluded 251 radar scans with 0 migration intensity, which were missing data for the crosswind component and altitude, and no RMSE, a measurement of error in the direction of migration across height bins. We also excluded two outlier observations in which bioscatter was moving at >200 m/s against the wind, which is biologically unrealistic and likely erroneous, as the maximum crosswind component is otherwise 78 m/s.

Magnetic Disturbance Index. Our hourly magnetic disturbance index, ΔBmax, measures the maximum change in the magnetic field in nanoTeslas (nT) relative to an expected baseline. This index is created from minute-resolution observations of the Earth's field as recorded at a set of observatories across North America (30). The raw observatory values are processed by the SuperMAG data center to remove quiet values (31), including the Earth's intrinsic field contribution and contributions from Solar Quiet (Sq) current systems in the ionosphere. The remaining signal, referred to widely as ΔB, represents magnetic perturbations from quiet conditions due to space weather effects. To create a value indicative of magnetic activity over longer periods, we took a rolling hourly maximum of the total vector magnitude of the disturbed field, resulting in a magnetometer-specific ΔBmax. Next, we linearly interpolated values to each radar observatory using Delaunay triangulation (59), yielding the final, station-specific index. The nearest magnetometer was always within 13° longitude and 12° latitude of the target radar station (*SI Appendix*, Fig. S1). We used all North American magnetometers available on SuperMAG between central Canada and Panama (Fig. 1*B*). Not all magnetometers were active throughout our entire study period and ΔBmax could not always be interpolated for all radar scans (*SI Appendix*, Fig. S2 and Table S1). In the end, we removed 6,188 and 3,494 radar scans in the fall and spring respectively with missing ΔBmax values from the final dataset. Our final datasets have 1,725,415 radar scans in the fall and 1,392,826 radar scans in the spring.

Our methodology allows for better characterization of local magnetic disturbances than standard global geomagnetic activity indices such as Kp, Dst, or the sunspot number (60–63). Ground magnetic perturbations can be highly localized, especially at higher latitudes (64) such that regional and global indices often miss local perturbations. The 3-hourly interval of the Kp index and low-latitude specificity of Dst can also miss mid-latitude signatures of substorms, which are localized to Earth's nightside with timescales of 3 h or less (65). Our index, ΔBmax, accounts for time and space localization of perturbations as best as possible. The occurrence of geomagnetic storms is closely correlated with the ~11-y solar cycle, which is defined by the cyclical appearance of sunspots (1). As a predictor, ΔBmax has a finer temporal resolution and allows for better temporal detrending than the sunspot number, which is measured daily and follows a cyclical trend. The sunspot number is additionally correlated with general solar activity and has been used in studies measuring the impact of radiofrequency noise on magnetoreception (17, 19). However, solar radiofrequency noise is thought to mostly impact the daylit side of the Earth (66) and the frequencies known to disrupt magnetoreception (67) might be filtered by Earth's ionosphere (68), which may decrease relevance for nocturnal migration.

Weather Data. We used east-west winds (u wind vector component; m/s), north-south winds (v wind vector component; m/s), air temperature (°C), pressure at mean sea-level (Pa), accumulated precipitation (kg/m^2), visibility (m), relative humidity (%), and total cloud cover (%) from the North American Regional Reanalysis (NARR) (69). Collectively, these variables are known to accurately predict bird migration behavior as measured with radar (26). Weather data are estimated for 3-hourly intervals in a 32-km grid, so each radar observation is associated with the closest NARR timestamp and grid block. Wind measurements (u wind, v wind) and air temperature were taken for each height bin in the radar air column, so we used the average across height bins. For the calculation of bird airspeed, the two vector components of the wind vector were subtracted from the bird groundspeed vector components (also in m/s), yielding bird airspeed vector components.

Modeling Framework. We used two complementary statistical frameworks to test our hypotheses. Our models control for the known effects of weather (above), temporal variables (specifically, decile of night, ordinal date, and year), and geographic variables (latitude and longitude) to measure putative effects of magnetic disturbances on bird migration. Our crosswind component and altitude models also include migration intensity as a predictor (with a cubic root transformation, instead of a log transformation, to avoid negative values), as these measures change with larger volumes of birds. Our models also use random effects and grouping variables to control for the temporal and spatial autocorrelation in our data (see below). All analyses were done in R version 4.2.0 (70). All predictor variables were centered and standardized using the "scale" function (70).

NLME Models. We built our mixed-effect models using the "lmer" function (package lme4) (36) and included nonlinear splines using the "bs" function (package "splines") (70). To build our models, we tested various random effect structures (see below) and included fixed effects of all weather, geographic and temporal variables. We tested random effects on models with an initial fixed effect structure in which all predictors had splines of three degrees of freedom except for time of night and day of year (which both had splines with five degrees of freedom) and latitude, longitude, and year (which had no splines, because they do not vary as much between observations). All models were fit with maximum likelihood to facilitate model comparison.

We tested the influence of the following random effects on model performance based on likely sources of autocorrelation in our data: 1) A "nightly" term that grouped each night of sampling from each radar station derived from the interaction of ordinal date, year, and radar station. This term included a random slope with a spline along time of night, both with and without a random intercept. This was our most important source of autocorrelation, as we expect measurements at each radar station for any given night to depend the most on each other. 2) A nightly term shared across radar stations from the interaction of ordinal date and year that also included a random slope with a spline along time of night, both with and without a random intercept. This accounts for larger sources of autocorrelation (e.g., weather) that might be shared across multiple radar stations on any given night. 3) A "seasonal" term from the interaction of year and radar station with a random slope and spline along ordinal date, also both with and without a random intercept. This accounts for between-day autocorrelation that might vary year to year and is unique to each radar station but is broadly tied to seasonality. 4) A random intercept for each radar station, accounting for geographic disparities unique to each station.

Our starting models only had the first random effect without random intercepts, and we sequentially tested and retained random slopes and random intercepts based on which caused the greatest reduction in AIC. Ultimately, models for all response variables and seasons converged to the same random effect structure, so we included all four random effects with random intercepts for all models.

We then fine-tuned spline complexity by iteratively testing each fixed effect a) without splines and b) with three to five degrees of freedom. We chose the degrees of freedom for each spline based on whether a model structure resulted in a lowered AIC. That is, we used AIC to specify whether an included variable should have a spline and the degrees of freedom of this spline. Default model convergence criteria were changed to a gradient norm of 0.1. Spline-selection models often ran into boundary issues with complex random effect structures, so for the purposes of spline selection, we simplified the random effect structure to include only a nightly term unique to each radar station with a random intercept and a seasonal term without a random intercept.

Once we finalized our "base" models for each season and response variable, we added all previously mentioned random effects and ΔBmax as a fixed main effect and with an interaction with cloud cover. In altitude models for both seasons and crosswind models for the fall, our models encountered singular boundaries in their random effects that were resolved by removing the random intercepts for the problematic random effects. We used log likelihood tests (function "anova") to test the explanatory value of models containing ΔBmax

compared to the base models. We then evaluated CI across values of ΔBmax to assess model support for predicted trends. We used the function "sim" (package "arm") (37) to generate 1,000 simulated fixed effect coefficients per model. We used the 0.025 and 0.975 quantiles to plot the 95% CI. When model CI were narrow enough around a trend such that the intervals did not overlap between the median ΔBmax (~17 nT) and the extremes, we considered the model to show strong support for the trend.

Gradient Boosted Decision Tree Models. We residualized our response variables using MLT models (function "xgb.train," package "xgboost") (38) built with our weather, geographic, and temporal variables. To avoid overfitting, we trained a model on a train dataset (70% of data, split randomly by unique days in each year) until new runs failed to further the model's explanatory power on a validation dataset (the remaining 30% of data) for 100 consecutive runs. We then fit a model on the complete dataset but restricted it to the number of runs identified with the validation dataset. Prior to running our final models, we fine-tuned the xgboost parameters by running models using a grid search using the training and validation sets. We kept the learning rate constant at 0.01, but varied gamma (values at 0, 1, 3, and and tree depth (values at 6, 8, 10, 12, 14, and 16, although we restricted our final tree depths to a maximum of 14 to ease run times). We stopped each model after 10 rounds in which the model failed to improve predictions on the validation dataset. We based our final parameter choice for each model on the parameter combination that produced the lowest model R^2, calculated as the covariance of the predicted results and the original validation dataset response variable divided by the variance of the original validation dataset response variable.

To examine associations between the residualized response variable and ΔBmax, we used least square regressions with robust covariance matrix estimated confidence bands (constructed with the R package "sandwich") (39, 40) with the interaction between unique day and year as a grouping variable. To test for the effect of interactions, we excluded the interacting variable from the xgboost residualization and included it with a spline and an interaction with ΔBmax in the regression with robust confidence bands. Model support was assessed similarly as with our NLME models.

Data, Materials, and Software Availability. Data and code for analyses are available at ref. 71. Code for the interpolation of ΔBmax is available at ref. 72.

ACKNOWLEDGMENTS. We thank T. Pegan, K. Wacker, M. Hack, A. Kimmitt, A. Benavides, M. Tingley, B. Tonelli, A. Farnsworth, A. Dokter, H. Mouritsen, H. Schmaljohann, J. McLaren, R. Muheim, and an anonymous reviewer for helpful comments and J. Megahan for contributing the illustration for Fig. 1*A*. This research depended on computational resources from the Advanced Research Computing at the University of Michigan, Ann Arbor. Access to NEXRAD radar data was provided by National Oceanic and Atmospheric Administration National Centers for Environmental Information. E.R.G.-C. was supported by National Science Foundation Graduate Research Fellowship Grant No. 2017247961 and a University of Michigan Rackham Merit Fellowship. B.M.V.D. was supported by a Cornell Presidential Postdoctoral Fellowship. M.B.M. was supported by National Science Foundation Grant AGS-1848724. B.M.W. and M.B.M. were supported by a University of Michigan MCubed grant.

Author affiliations: [a]Department of Ecology and Evolutionary Biology, University of Michigan, Ann Arbor, MI 48109; [b]Museum of Zoology, University of Michigan, Ann Arbor, MI 48109; [c]Cornell Lab of Ornithology, Cornell University, Ithaca, NY 14850; [d]Department of Physics, University of Texas, Arlington, TX 76019; [e]Department of Fish, Wildlife, and Conservation Biology, Colorado State University, Fort Collins, CO 80523; [f]Department of Statistics, University of Michigan, Ann Arbor, MI 48109; and [g]Climate and Space Sciences and Engineering, University of Michigan, Ann Arbor, MI 48109

1. E. W. Cliver, Solar activity and geomagnetic storms: The first 40 years. *Eos* **75**, 569–584 (1994).
2. M. Moldwin, *An Introduction to Space Weather* (Cambridge University Press, 2008).
3. L. J. Lanzerotti, "Space weather effects on technologies" in *Space Weather*, P. Song, H. J. Singer, G. L. Siscoe, Eds. (Geophysical Monograph Series, AGU, 2001), pp. 11–22.
4. S. E. Fick, R. J. Hijmans, WorldClim 2: New 1-km spatial resolution climate surfaces for global land areas. *Int. J. Climatol.* **37**, 4302–4315 (2017).
5. H. Mouritsen, Long-distance navigation and magnetoreception in migratory animals. *Nature* **558**, 50–59 (2018).
6. W. Wiltschko, R. Wiltschko, Magnetic compass of European robins. *Science* **176**, 62–64 (1972).
7. N. Chernetsov *et al.*, Migratory Eurasian Reed Warblers can use magnetic declination to solve the longitude problem. *Curr. Biol.* **27**, 2647–2651 (2017).
8. J. Wynn, O. Padget, H. Mouritsen, C. Perrins, T. Guilford, Natal imprinting to the Earth's magnetic field in a pelagic seabird. *Curr. Biol.* **30**, 1–5 (2020).
9. J. Wynn *et al.*, Magnetic stop signs signal a European songbird's arrival at the breeding site after migration. *Science* **375**, 446–449 (2022).
10. J. R. Brothers, K. J. Lohmann, Evidence for geomagnetic imprinting and magnetic navigation in the natal homing of sea turtles. *Curr. Biol.* **25**, 392–396 (2015).
11. D. Kishkinev, N. Chernetsov, A. Pakhomov, D. Heyers, H. Mouritsen, Eurasian reed warblers compensate for virtual magnetic displacement. *Curr. Biol.* **25**, R811–R826 (2015).
12. F. R. Moore, Geomagnetic disturbance and the orientation of nocturnally migrating birds. *Science* **196**, 682–684 (1977).
13. E. Rakhimberdiev *et al.*, Naïve migrants and the use of magnetic cues: temporal fluctuations in the geomagnetic field differentially affect male and female Ruff *Philomachus pugnax* during their first migration. *Ibis* **156**, 864–869 (2014).
14. W. J. Richardson, Autumn migration over Puerto Rico and the western Atlantic: A radar study. *Ibis* **118**, 309–332 (1976).
15. W. T. Keeton, T. S. Larkin, D. M. Windsor, Normal fluctuations in the Earth's magnetic field influence pigeon orientation. *J. Comp. Physiol.* **95**, 95–103 (1974).
16. I. Schiffner, R. Wiltschko, Temporal fluctuations of the geomagnetic field affect pigeons' entire homing flight. *J. Comp. Physiol. A* **197**, 765–772 (2011).
17. B. A. Tonelli, C. Youngflesh, M. W. Tingley, Geomagnetic disturbance associated with increased vagrancy in migratory landbirds. *Sci. Rep.* **13**, 414 (2023).
18. G. Bianco, M. Ilieva, S. Åkesson, Magnetic storms disrupt nocturnal migratory activity in songbirds. *Biol. Lett.* **15**, 20180918 (2019).
19. J. Granger, L. Walkowicz, R. Fitak, S. Johnsen, Gray whales strand more often on days with increased levels of atmospheric radio-frequency noise. *Curr. Biol.* **30**, R155–R156 (2020).
20. B. Schreiber, O. Rossi, Correlation between magnetic storms due to solar spots and pigeon homing performances. *IEEE Trans. Magn.* **14**, 961–963 (1978).
21. K. P. Able, Geomagnetic disturbance and migratory bird orientation: Is there an effect? *Anim. Behav.* **35**, 599–601 (1987).
22. B. R. Moore, Magnetic fields and orientation in homing pigeons: Experiments of the late W. T. Keeton. *Proc. Natl. Acad. Sci. U.S.A.* **85**, 4907–4909 (1988).
23. A. Farnsworth *et al.*, A characterization of autumn nocturnal migration detected by weather surveillance radars in the northeastern USA. *Ecol. Appl.* **26**, 752–770 (2016).
24. S. Bauer *et al.*, The grand challenges of migration ecology that radar aeroecology can help answer. *Ecography* **42**, 861–875 (2019).
25. K. G. Horton *et al.*, Nocturnally migrating songbirds drift when they can and compensate when they must. *Sci. Rep.* **6**, 21249 (2016).
26. B. M. Van Doren, K. G. Horton, A continental system for forecasting bird migration. *Science* **361**, 1115–1118 (2018).
27. T. Alerstam, Why do migrating birds fly along coastlines? *J. Theor. Biol.* **65**, 699–712 (1977).
28. T. C. Williams, J. M. Williams, P. G. Williams, P. Stokstad, Bird migration through a mountain pass studied with high resolution radar, ceilometers, and census. *Auk* **118**, 389–403 (2001).
29. K. G. Horton *et al.*, Navigating north: How body mass and winds shape avian flight behaviours across a North American migratory flyway. *Ecol. Lett.* **21**, 1055–1064 (2018).
30. J. W. Gjerloev, A global ground-based magnetometer initiative. *EOS* **90**, 230–231 (2009).
31. J. W. Gjerloev, The SuperMAG data processing technique. *J. Geophys. Res. Sp. Phys.* **117**, A09213 (2012).
32. W. J. Richardson, "Timing of bird migration in relation to weather: Updated review" in *Bird Migration: Physiology and Ecophysiology*, E. Gwinner, Ed. (Springer-Verlag, ed. 1, 1990), pp. 78–101.
33. W. T. Keeton "Effects of magnets on pigeon homing" in *Animal Orientation and Navigation*, S. R. Galler, K. Schmidt-Koenig, G. J. Jacobs, R. E. Belleville, Eds. (NASA Washington, DC, 1972), pp. 579–594.
34. S. T. Emlen, N. J. Demong, "Orientation strategies used by free-flying bird migrants: A radar tracking study" in *Animal Migration, Navigation and Homing* (Springer Berlin Heidelberg, 1978), pp. 283–293.
35. T. Alerstam, Bird migration across a strong magnetic anomaly. *J. Exp. Biol.* **130**, 63–86 (1987).
36. D. Bates, M. Mächler, B. M. Bolker, S. C. Walker, Fitting linear mixed-effects models using lme4. *J. Stat. Softw.* **67**, 1–48 (2015).
37. A. Gelman, Y.-S. Su, arm: Data analysis using regression and multilevel/hierarchical models (2021). CRAN. https://CRAN.R-project.org/package=arm. Accessed 28 August 2022.
38. T. Chen, C. Guestrin, "XGBoost: A scalable tree boosting system" in *Proceedings of the 22nd ACM SIGKDD International Conference on Knowledge Discovery and Data Mining*, B. Krishnapuram *et al.*, Eds. (Association for Computing Machinery, New York, 2016), pp. 785–794.
39. A. Zeileis, Econometric computing with HC and HAC covariance matrix estimators. *J. Stat. Softw.* **11**, 1–17 (2004).
40. A. Zeileis, S. Köll, N. Graham, Various versatile variances: An object-oriented implementation of clustered covariances in R. *J. Stat. Softw.* **95**, 1–36 (2020).
41. K. P. Able, Field studies of avian nocturnal migratory orientation I. Interaction of sun, wind and stars as directional cues. *Anim. Behav.* **30**, 761–767 (1982).
42. K. Thorup *et al.*, Evidence for a navigational map stretching across the continental U.S. in a migratory songbird. *Proc. Natl. Acad. Sci. U.S.A.* **104**, 18115–18119 (2007).
43. A. C. Perdeck, Two types of orientation in migrating starlings, *Sturnus vulgaris* L., and chaffinches, *Fringilla coelebs* L., as revealed by displacement experiments. *Ardea* **46**, 1–37 (1958).
44. U. Munro, J. A. Munro, J. B. Phillips, R. Wiltschko, W. Wiltschko, Evidence for a magnetite-based navigational "map" in birds. *Naturwissenschaften* **84**, 26–28 (1997).
45. C. Nilsson, R. H. G. Klaassen, T. Alerstam, Differences in speed and duration of bird migration between spring and autumn. *Am. Nat.* **181**, 837–845 (2013).
46. H. Schmaljohann, Proximate mechanisms affecting seasonal differences in migration speed of avian species. *Sci. Rep.* **8**, 1–10 (2018).
47. F. A. La Sorte, D. Fink, W. M. Hochachka, S. Kelling, Convergence of broad-scale migration strategies in terrestrial birds. *Proc. R. Soc. B* **283**, 20152588 (2016).
48. T. Alerstam, Wind as selective agent in bird migration. *Ornis Scand.* **10**, 76–93 (1979).

49. W. D. Gonzalez *et al.*, What is a geomagnetic storm? *J. Geophys. Res.* **99**, 5771–5792 (1994).
50. L. Kepko *et al.*, Substorm current wedge revisited. *Space Sci. Rev.* **190**, 1–46 (2015).
51. B. T. Tsurutani, W. D. Gonzalez, "Magnetic storms" in *From the Sun: Auroras, Magnetic Storms, Solar Flares, Cosmic Rays* (American Geophysical Union Washington, DC, 1960), pp. 57–66.
52. W. H. Campbell, Annual and semiannual changes of the quiet daily variations (Sq) in the geomagnetic field at North American locations. *J. Geophys. Res.* **87**, 785–796 (1982).
53. Kakioka Magnetic Observatory, Kakioka Geomagnetic Storm Catalog (2015). Kakioka Magnetic Observatory Digital Data Service. https://doi.org/10.48682/386bd.007b0. Accessed 12 June 2023.
54. W. J. Sutherland, Evidence for flexibility and constraint in migration systems. *J. Avian Biol.* **29**, 441–446 (1998).
55. D. H. Hathaway, The solar cycle. *Living Rev. Sol. Phys.* **12**, 1–87 (2015).
56. K. G. Horton *et al.*, Phenology of nocturnal avian migration has shifted at the continental scale. *Nat. Clim. Chang.* **10**, 63–68 (2020).
57. T.-Y. Lin *et al.*, MistNet: Measuring historical bird migration in the US using archived weather radar data and convolutional neural networks. *Methods Ecol. Evol.* **10**, 1908–1922 (2019).
58. P. B. Chilson *et al.*, Estimating animal densities in the aerosphere using weather radar: To Z or not to Z? *Ecosphere* **3**, 72 (2012).
59. W. H. Press, S. A. Teukolsky, W. T. Vetterling, B. P. Flannery, *Numerical Recipes 3rd Edition: The Art of Scientific Computing* (Cambridge University Press, ed. 3, 2007).
60. J. Bartels, N. H. Heck, H. F. Johnston, The three-hour range index measuring geomagnetic activity. *J. Geophys. Res.* **44**, 411–454 (1938).
61. M. Sugiura, *Hourly Values of Equatorial Dst for the IGY* (Pergamon Press, 1964).
62. G. Rostoker, Geomagnetic indices. *Rev. Geophys. Sp. Phys.* **10**, 935–950 (1972).
63. M. Menvielle, T. Iyemori, A. Marchaudon, M. Nosé, "Geomagnetic indices" in *Geomagnetic Observations and Models*, M. Mandea, M. Korte, Eds. (Springer Dordrecht, ed. 1, 2010), pp. 182–228.
64. C. M. Ngwira *et al.*, A study of intense local dB/dt variations during two geomagnetic storms. *Space Weather* **16**, 676–693 (2018).
65. R. L. McPherron, X. Chu, The midlatitude positive bay index and the statistics of substorm occurrence. *J. Geophys. Res. Sp. Phys.* **123**, 2831–2850 (2018).
66. M. H. MacAlester, W. Murtagh, Extreme space weather impact: An emergency management perspective. *Space Weather* **12**, 530–537 (2014).
67. S. Engels *et al.*, Anthropogenic electromagnetic noise disrupts magnetic compass orientation in a migratory bird. *Nature* **509**, 353–356 (2014).
68. J. J. Condon, S. M. Ransom, *Essential Radio Astronomy* (Princeton University Press, ed. 1, 2016).
69. F. Mesinger *et al.*, North American regional reanalysis. *Bull. Am. Meteorol. Soc.* **87**, 343–360 (2006).
70. R Core Team, R: A Language and Environment for Statistical Computing, v. 4.2.0 (R Foundationfor Statistical Computing, Vienna, Austria, 2022). https://www.r-project.org/.
71. E. R. Gulson-Castillo, Space weather disrupts nocturnal bird migration [Data set]. Zenodo. https://doi.org/10.5281/zenodo.8319741. Deposited 5 September 2023.
72. M. X. Bui, D. T. Welling, spacecataz/BirdBeaks: Results version for PNAS publication (v0.1). Zenodo. https://doi.org/10.5281/zenodo.8302156. Deposited 30 August 2023.